The EUMETSAT Satellite Application Facility on Land Surface Analysis

Product User Manual

Vegetation Parameters (VEGA)

PRODUCTS: LSA-421 (MDFVC), LSA-422 (MTFVC), LSA-450 (MTFVC-R), LSA-423 (MDLAI), LSA-424 (MTLAI), LSA-451 (MTLAI-R), LSA-425 (MDFAPAR), LSA-426 (MTFAPAR), LSA-452 (MTFAPAR-R)

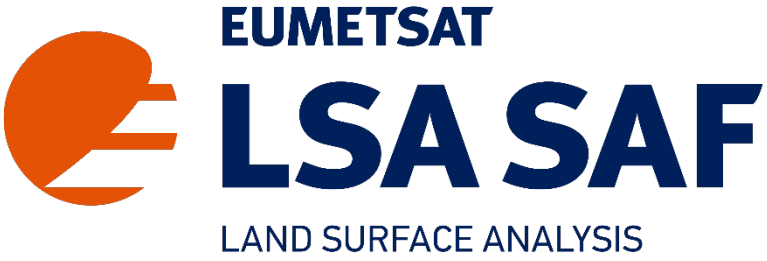

Reference Number: SAF/LAND/UV/PUM_VEGA/3.2
Issue/Revision Index: Version 3.2
Last Change: 06/03/2018

DOCUMENT SIGNATURE TABLE

	Name	Date	Signature
Prepared by :	F.J. García-Haro, F. Camacho, M. Campos-Taberner, J. Sanchez-Zapero, B. Martínez, M.A. Gilabert		
Approved by :	Land SAF Project Manager (IPMA)		

DOCUMENTATION CHANGE RECORD

Issue / Revision	Date	Description :
Version 2.0	15/02/2007	Version prepared for the ORR-2
Version 2.1	15/01/2008	Version prepared for the ORR-2 Close-out
Version 2.1/2	10/12/2011	Updated version including 10-day VEGA products
Version 2.1/3	8/11/2013 (25/11/2013)	Updated version (v2.1) prepared for the VEGA-10 ORR (revised version)
Version 2.1/4	11/12/2013	Updated version modified following the recommendations of the ORR Review Board.
Version 3.0	24/02/2016	Updated version (v3.0) modified for the reprocessing chain, including changes made to version 2 of FVC (LSA-421 and LSA-422), LAI (LSA-423 and LSA-424), and FAPAR (LSA-425 and LSA-426) products. This revised version has taken into account the PCR/ORR recommendations.
Version 3.1	18/07/2017	The same version (v3.0) but applicable also to the reprocessed CDR: LSA-450 (MTFVC-R), LSA-451 (MTLAI-R), LSA-452 (MTFAPAR-R).
Version 3.2	06/02/2018	Reviewed version modified following the recommendations of the DRR Review Board.

TABLE OF CONTENTS

List of Figures

List of Tables

1 Introduction

The Satellite Application Facility (SAF) on Land Surface Analysis (LSA) is part of the SAF Network, a set of specialised development and processing centres, serving as EUMETSAT (European organization for the Exploitation of Meteorological Satellites) distributed Applications Ground Segment. The SAF network complements the product-oriented activities at the EUMETSAT Central Facility in Darmstadt. The main purpose of the LSA SAF is to take full advantage of remotely sensed data, particularly those available from EUMETSAT sensors, to measure land surface variables, which will find primarily applications in meteorology (http://landsaf.ipma.pt).

The spin-stabilised Meteosat Second Generation (MSG) has an imaging-repeat cycle of 15 minutes. The Spinning Enhanced Visible and Infrared Imager (SEVIRI) radiometer embarked on the MSG platform encompasses unique spectral characteristics and accuracy, with a 3 km resolution (sampling distance) at nadir (1km for the high-resolution visible channel), and 12 spectral channels (Schmetz et al. 2002).

Several studies have stressed the role of land surface processes on weather forecasting and climate modelling (e.g. Dickinson et al. 1983, Mitchell et al. 2004, Ferranti and Viterbo 2006). The LSA SAF has been especially designed to serve the needs of the meteorological community, particularly Numerical Weather Prediction (NWP). However, there is no doubt that the LSA SAF addresses a much broader community, which includes users from:

- Weather forecasting and climate modelling, requiring detailed information on the nature and properties of land.
- Environmental management and land use, needing information on land cover type and land cover changes (e.g. provided by biophysical parameters or thermal characteristics).
- Agricultural and Forestry applications, requiring information on incoming/outgoing radiation and vegetation properties.
- Renewable energy resources assessment, particularly biomass, depending on biophysical parameters, and solar energy.
- Natural hazards management, requiring frequent observations of terrestrial surfaces in both the solar and thermal bands.
- Climatological applications and climate change detection, requiring long and homogeneous time-series.

Table 1. The LSA SAF Set of Products and respective sensors and platforms. The table covers both existing and future EUMETSAT satellites, and therefore refers operational products and development activities.

Product Family	Product Group	Sensors/Platforms
Radiation	Land Surface Temperature (LST)	SEVIRI/MSG, AVHRR/Metop, FCI/MTG, VII/EPS-SG

	Land Surface Emissivity (EM)	SEVIRI/MSG, FCI/MTG (internal product for other sensors)
	Land Surface Albedo (AL)	SEVIRI/MSG, AVHRR/Metop, FCI/MTG, VII/EPS-SG, 3MI/EPS-SG
	Down-welling Short-wave Fluxes (DSSF)	SEVIRI/MSG, FCI/MTG
	Down-welling Long-wave Fluxes (DSLF)	SEVIRI/MSG, FCI/MTG
Vegetation	Normalized Difference Vegetation Index (NDVI)	AVHRR/Metop, VII/EPS-SG
	Fraction of Vegetation Cover (FVC)	SEVIRI/MSG, AVHRR/Metop, FCI/MTG, VII/EPS-SG, 3MI/EPS-SG
	Leaf Area Index (LAI)	SEVIRI/MSG, AVHRR/Metop, FCI/MTG, VII/EPS-SG, 3MI/EPS-SG
	Fraction of Absorbed Photosynthetically Active Radiation (FAPAR)	SEVIRI/MSG, AVHRR/Metop, FCI/MTG, VII/EPS-SG, 3MI/EPS-SG
	Gross Primary Production (GPP)	SEVIRI/MSG, FCI/MTG
	Canopy Water Content (CWC)	AVHRR/Metop, VII/EPS-SG
Energy Fluxes	Evapotranspiration (ET)	SEVIRI/MSG, FCI/MTG
	Reference Evapotranspiration (ET0)	SEVIRI/MSG, FCI/MTG
	Surface Energy Fluxes: Latent and Sensible (LE&H)	SEVIRI/MSG, FCI/MTG
Wild Fires	Fire Detection and Monitoring (FD&M)	SEVIRI/MSG
	Fire Radiative Power	SEVIRI/MSG, FCI/MTG, VII/EPS-SG
	Fire Radiative Energy and Emissions (FRE)	SEVIRI/MSG, FCI/MTG, VII/EPS-SG
	Fire Risk Map (FRM)	SEVIRI/MSG, FCI/MTG
	Burnt Area (BA)	AVHRR/Metop, VII/EPS-SG

The LSA SAF products are based on level 1.5 SEVIRI/Meteosat and/or level 1b MetOp data. Forecasts provided by the European Centre for Medium-range Weather Forecasts (ECMWF) are also used as ancillary data for atmospheric correction.

The SEVIRI/Meteosat 0 degree image service derived products, are generated for 4 different geographical areas within Meteosat disk (Figure 1) as well as in a single MSG-Disk product covering the full the Meteosat disk.

- Euro – Europe, covering all EUMETSAT member states;
- NAfr – Northern Africa encompassing the Sahara and Sahel regions, and part of equatorial Africa.
- SAfr – Southern Africa covering the African continent south of the Equator.
- SAme – South American continent within the Meteosat disk.

MetOp derived parameters are currently available at level 1b full spatial resolution and for the processed Product Distribution Units (PDUs), each corresponding to about 3 minutes of instrument-specific observation data.

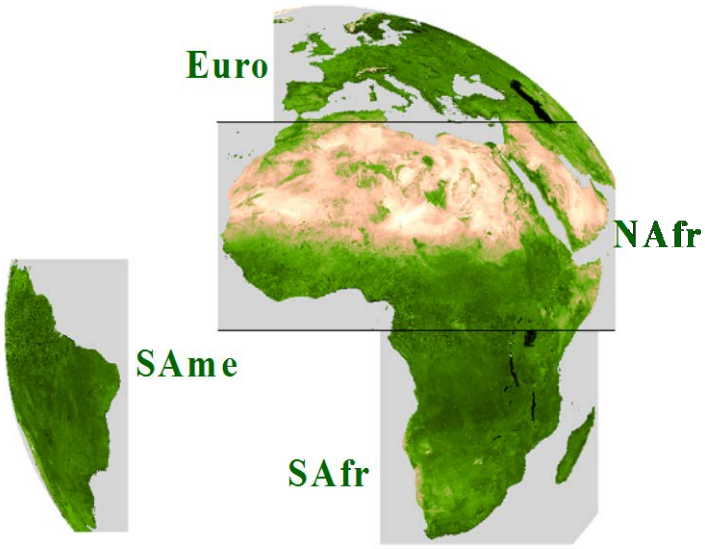

Figure 1. The LSA SAF geographical areas.

The LSA SAF system is fully centralized at IPMA and will be able to operationally generate, archive, and disseminate the operational products. The monitoring and quality control of the operational products, also centralized at IPMA, is performed automatically by the LSA SAF software, which provides quality information to be distributed with the products. The LSA SAF products are currently available from LSA SAF website (http://landsaf.ipma.pt) that contains real time examples of the products as well as updated information.

This document is one of the product manuals dedicated to LSA SAF users. The algorithm and the main characteristics of the daily (MDFVC, MDLAI and MDFAPAR) and ten-day (MTFVC, MTLAI and MTFAPAR) VEGA products generated by the LSA SAF system are described in the following sections. The characteristics of SEVIRI based VEGA products provided by the LSA SAF are described in Table 2.

Table 2. Product Requirements for MSG VEGA products, in terms of area coverage, resolution and accuracy.

			Resolution		Accuracy		
Product	**Identifier**	**Coverage**	**Temporal**	**Spatial**	**Optimal**	**Target**	**Threshold**
MDFVC	LSA-401	MSG disk	1-day	MSG pixel	Max [0.05,10%]	Max [0.075,15%]	Max [0.1,20%]
MTFVC	LSA-402	MSG disk	10-days	MSG pixel	Max [0.05,10%]%	Max [0.075,15%]	Max [0.1,20%]
MDLAI	LSA-404	MSG disk	1-day	MSG pixel	15%	Max [0.5,20%]	Max [0.75,25%]
MTLAI	LSA-405	MSG disk	10-days	MSG pixel	15%	Max [0.5,20%]	Max [0.75,25%]
MDFAPAR	LSA-407	MSG disk	1-day	MSG pixel	Max [0.05,10%]	Max [0.075,15%]	Max [0.1,20%]
MTFAPAR	LSA-408	MSG disk	10-days	MSG pixel	Max [0.05,10%]	Max [0.075,15%]	Max [0.1,20%]

2 Algorithm

2.1 Introduction

The FVC (Fractional Vegetation Cover), the LAI (Leaf Area Index) and the FAPAR (Fraction of Absorbed Photosynthetically Active Radiation) are key variables for a wide range of land biosphere applications. The FVC represents the fraction of green vegetation covering a unit area of horizontal soil. The LAI is a quantitative measure of the amount of live green leaf material present in the canopy per unit ground surface. Specifically, LAI is a dimensionless variable [m^2/m^2] defined as one half the total leaf area per unit ground area and accounts for the surface of leaves contained in a vertical column normalized by its cross-sectional area. For non-leaves vegetation types, such as needles trees, LAI can be expressed as the total foliage surface area per unit of horizontally projected ground surface area. The FAPAR represents the fraction of photosynthetically active radiation (400-700 nm) absorbed by the green parts of the canopy, and therefore constitutes an indicator of the presence and productivity of live vegetation. FAPAR depends both on canopy structure, leaf and soil optical properties and irradiance conditions.
For fully and healthy developed canopies, LAI indicates the amount of green vegetation that absorbs or scatters the solar radiation. It represents the interface between the soil background and the atmosphere for the energy and mass exchanges. The scaling effect may cause biophysical retrieval from coarse resolution sensor data to differ from the arithmetic average of values derived independently from fine resolution sensor data (Wu and Zhao-Liang, 2009). The scaling effect is quite important for LAI and only marginal for FVC because this latter is quasi-linearly related to the reflectance (Malingreau and Belward 1992, Weiss et al. 2000).
FVC is mandatory for a thorough description of land surface processes in the surface parameterisation schemes implemented in the climate and weather forecasting models. FVC is generally close to FAPAR with the advantage of being defined independently of illuminations conditions making it an intrinsic canopy attribute. Besides, the FVC is relevant for a wide range of Land Biosphere Applications such as agriculture and forestry, environmental management and

land use, hydrology, natural hazards monitoring and management, vegetation-soil dynamics monitoring, drought conditions and fire scar extent. The LAI is a key input of Numerical Weather Prediction (NWP) models, regional and global climate modelling, weather forecasting and global change monitoring. Besides, the LAI is relevant for Land Biosphere Applications such as agriculture and forestry, environmental management and land use, hydrology, natural hazards monitoring and management, vegetation-soil dynamics monitoring and drought conditions. FAPAR is a key variable in models assessing vegetation primary productivity and, more generally, in carbon cycle models implementing up-to-date land surfaces process schemes (e.g. Sellers et al. 1997). Besides, it is an indicator of the health of vegetation.

FVC, LAI and FAPAR are used extensively to represent vegetation abundance and canopy structure and reflect changes in vegetation from global to local scales because they echo to rapid changes in climatic conditions or environmental stress factors. For effective use in coarse scale models, these variables must be collected over a long period of time (decades) and for all ecosystems of the terrestrial surface. To resolve rapid changes of vegetation status and amount under both the influence of climate and human activities, relatively high frequency observations are required, currently provided by the SEVIRI instrument.

The algorithm for retrieving FVC and LAI relies on optimised Spectral Mixture Analysis (SMA) methods in which endmember signatures are no longer treated as constants, but they are represented by multi-modal probability density functions. The use of standardized SMA improves understanding of the impact of endmember variability on the derivation of subpixel vegetation fractions at a global scale. The LAI is estimated from a FVC using a semiempirical approach as in Roujean and Lacaze (2002). This method relies on a tractable physical model for interception of solar irradiance by vegetative canopies. A statistical approach is proposed for retrieving daily FAPAR from BRDF data, corrected of surface's reflectance anisotropy and minimising the effect of soil reflectance (Roujean and Bréon, 1995). The LSA SAF methodology has been applied to different remotely sensed data, including SPOT/VEGETATION, MODIS and Sentinel-2 like data, showing good performances (García-Haro et al. 2006, Verger et al. 2007, 2009a,2009b, Camacho et al. 2013).

The current algorithm (v3.0) version was integrated in early 2016. It should be noted that while FVC and LAI algorithms were modified in version 3.0, FAPAR algorithm was not modified in version 3.0 (i.e. FAPAR v2.1=FAPAR v3.0). Details about the improvements between versions 2.1 and 3.0 are provided in the dedicated section 3.5.

2.2 Algorithm inputs

The technical properties of final products of FVC, LAI and FAPAR (spatial and temporal resolution, thematic accuracy, etc.) depend on the input data, and the retrieval algorithms. Rather than using reflectance, the algorithm uses as input the directional coefficients of the BRDF model (HDF5_LSASAF_MSG_AL-Channel-K012 for daily estimates or HDF5_LSASAF_MSG_AL-Channel-K012-D10 for the 10-day products) for the different spectral channels (Geiger et al. 2008). This is an internal product derived as a component of the albedo algorithm (SAF/LAND/MF/PUM_Al/1.6v2). Model coefficients result from simulating the BRDF following the general expression presented by Roujean et al. (1992):

$$R(\theta_v, \theta_s, \phi) = k_0 + k_1 f_1(\theta_v, \theta_s, \phi) + k_2 f_2(\theta_v, \theta_s, \phi) \quad (1)$$

where θ_v, θ_s, ϕ stand for the sun zenith, view zenith and relative azimuth angles, respectively, and f_1, f_2 stand for the geometric and volume scattering kernels, respectively.

The negative impact due to view/sun angles variations in surface reflectance are thus minimized because the products are derived using the same geometry for the whole SEVIRI disk. While the FVC and LAI products rely only on the k0 BRDF parameter, the FAPAR relies on the use of the three BRDF parameters (i.e., k_0, k_1, and k_2) (see Figure 2). Inputs for retrieving FVC are thus atmospherically corrected cloud-cleared TOC k0 parameters (Daily, 10-Day) in the three relevant SEVIRI spectral channels: red (VIS-0.6), near-infrared, NIR (VIS-0.8) and middle-infrared, MIR (IR-1.6). Note that the usual SEVIRI naming convention for these channels is 0.6-visual, 0.8-visual, and 1.6- near-infrared. Physically the k_0 parameters correspond to isotropic reflectance, i.e. reflectance factor values directionally normalized to reference illumination and observation zenith angles of 0°. This geometry leads to a minimum contribution of the shadow proportion (hotspot geometry) and a physically correct estimation of FVC (Roujean and Lacaze 2002), coinciding with the complement to unity of the gap fraction at nadir direction. Estimating the FVC with increased values of the sun zenith would lead to an overestimation of FVC. At this geometry, however, the contribution of illuminated soil background is significant, constituting thus a source of "noise" that has long been recognized as major problem in remote sensing of vegetation (e.g. Huete et al. 1988).

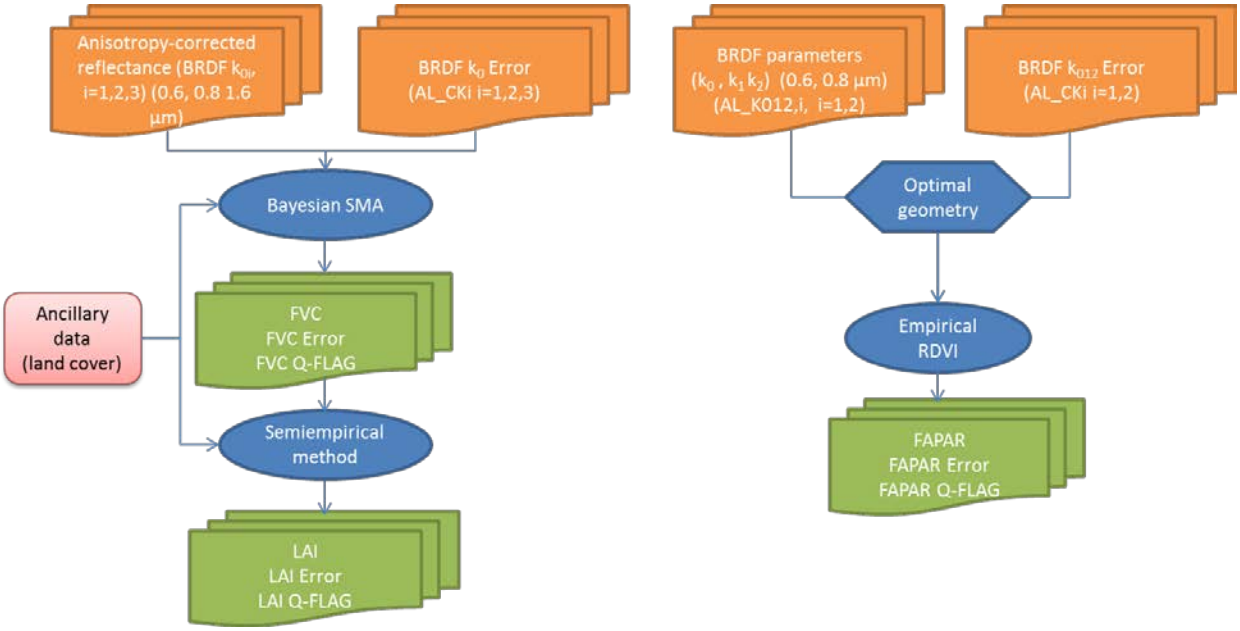

Figure 2. Flow chart of the algorithm for FVC, LAI and FAPAR determination.

Inputs for retrieving FAPAR (see figure 2) are atmospherically corrected cloud-screened TOC k_i parameters **(**Daily, 10-Day**)** in two SEVIRI channels: red (VIS-0.6) and near-infrared, NIR (VIS-0.8). Note that the VEGA algorithms of the daily products and the 10-day products are identical. Note that the VEGA algorithms of the daily products and the 10-day products are identical. Hence, the VEGA ten-day differs of VEGA daily products only in the BRDF input (daily and 10-day, respectively). Comments regarding the temporal characteristics and spatial coverage of the albedo products therefore also apply to the vegetation products. In order to reduce the sensitivity of the resulting daily estimates to reflectance outliers and extended periods of missing data because of

persistent cloudiness, it is necessary to combine the information over a longer time period. A recursive scheme is applied for this purpose. The daily albedo product is computed using an iterative scheme with a characteristic time scale of five days. By contrast, the 10-day albedo product is currently a classic composite expanding over a 30-day period. (we refer to section 4.5.3 of SAF/LAND/MF/ATBD_ETAL/1.3).
Hence, the VEGA ten-day differs of VEGA daily products only in the BRDF input. The quality of the SEVIRI BRDF parameters has been addressed in a related document (SAF/LAND/UV/VEGA_VR/2.1-5). Problematic areas with large BRDF uncertainty values correspond to high latitudes over Europe and in South America. k_2 BRDF product presents generally the largest uncertainties as well as noisy profiles on a short time scale (only for daily products) in other regions, particularly in Western Africa and regions in the south hemisphere. The quality of the FAPAR is directly related to the BRDF quality, whereas FVC and LAI uncertainties are associated to the quality of k_0.

2.3 FVC Algorithm description

The traditional SMA assumes that each mixture pixel **r** $(r_1,r_2,...,r_n)$, where n is the total number of bands, can be approximated by a linear mixture of endmember reflectances **E** weighted by their corresponding fractional proportions **f**:

$$\mathbf{r} = \mathbf{E}\,\mathbf{f} + \boldsymbol{\varepsilon} \qquad (2)$$

where **E** [$n \times c$] is the matrix of endmembers, **f** is a vector with the *c* unknown proportions in the mixture, and **ε** is the residual vector.

The coarse spatial resolution of SEVIRI data poses a significant challenge for endmember selection in traditional SMA. The algorithm assumes that each unknown pixel can be modelled by those candidate models (i.e. pairs of vegetation and soil subclasses) which are compatible with the SMA assumptions (i.e. they should lie on the "extended convex hull" defined by the model). A brief summary of the main algorithm steps is now given.

The first step consists in generating an adequate characterization of the variability of the pure components. Soil (bare soil, rock) and vegetation (dense crops, and forests) classes are represented by a large number of training set of pixels, making use of the very detailed information from different data sources (land cover classifications and other validated biophysical products, including finer spatial resolution data). The vegetation and soil components are then modeled using a mixture model weighted sum of Gaussian distributions to determine the mean vector μ_k and covariance matrix Σ_k for the Gaussians clusters $\phi_k(\mathbf{x} \mid \mu_k, \Sigma_k)$

$$f_j(\mathbf{x} \mid \mu_{jk}, \Sigma_{jk}) = \sum_{k=1}^{G_j} \tau_k \phi_k(\mathbf{x} \mid \mu_{jk}, \Sigma_{jk}) \qquad \text{j = s, v} \qquad (3)$$

where τ_k is the probability that an observation belongs to the *k*-th component ($\tau_k \geq 0$; $\sum_{k=1}^{G_j} \tau_k = 1$).

The algorithm computes all possible models by taking all possible pairs $M_K \equiv (f_{veg(k)}, f_{soil(k')})$. Let $\pi(M_K)$ be the *a priori* probability of having the model M_k at a particular pixel. The basic idea is

that the posterior probability or membership of model M_K given pixel data **r**, namely $p(M_K|\mathbf{r})$, is proportional to the probability of the data given model M_k, namely $p(\mathbf{r}|M_K)$, times the model's prior probability $\pi(M_K)$:

$$p(M_K|\mathbf{r}) = \frac{p(\mathbf{r}|M_K)\cdot\pi(M_K)}{\sum_{i=1}^{N} p(\mathbf{r}|M_i)\cdot\pi(M_i)} \quad (4)$$

The fractions of soil and vegetation are then calculated using the formulation of García-Haro et al. (1996), which provides a unique and unbiased solution that is computationally fast. Let FVC(M_K) be the fraction of vegetation obtained using the M_K model. FVC is estimated as a linear combination of single-model estimates:

$$FVC = \sum_{k=1}^{N} p(M_k|\mathbf{r})\cdot FVC(M_k) \quad (5)$$

In this sum, the contribution of each model is weighted by its Bayesian *a posteriori* probability $p(M_K|\mathbf{r})$. The algorithm performs a standardisation on both the endmember and the image spectra as a previous step before applying the SMA (García-Haro et al. 2005a). Through this standardization, SMA is less sensitive the brightness variability within each vegetation-soil component, at reducing the influence of external factors such as shading, brightness differences due to variability of surface roughness and terrain illumination.

The last step consists in assessing the statistical confidence intervals of FVC predictions, Err(FVC), taking into account two different sources of error, namely propagation of input errors (ε_{SMA}) and uncertainty due to model selection (ε_{model}):

$$Err(FVC) = \sqrt{\varepsilon_{SMA}^2 + \varepsilon_{model}^2} \quad (6)$$

The impact of input errors, Err(k_0), on the prediction of FVC (ε_{SMA}) is assessed statistically taking into account from the usual error propagation laws as in the classical Spectral Mixture Analysis method (García-Haro et al. 1996). The second source of error (ε_{model}) is due to the dispersion (variance) of the possible solutions.

2.4 LAI Algorithm description

The solution of the radiative transfer problem can be reduced to the problem of diffuse transmission of the solar radiation by a medium of finite optical thickness. Assuming that leaves are flat with bi-Lambertian properties (reflectances and transmittance are isotropic), the following simplified form is proposed for the fraction of solar radiation intercepted by the vegetation (FIPAR):

$$FIPAR(\theta_s) = 1 - T(\theta_s) = 1 - \exp[-b(G(\theta_s)/\mu_s)\Omega LAI] \quad (7)$$

where $\mu_s = cos\theta_s$, being θ_s the solar zenith angle, $G(\theta_s)$ is the average extinction function (Ross 1981), the backscattered parameter, b, is assumed equal to 0.945 for all vegetation (Roujean et al. 1997), Ω is the clumping index (Nilson 1971) which accounts for the degree of dependence of the vegetation stands position. When the sun and the observer are both at zenith, FVC is equivalent to

the FIPAR (Smith et al. 1993). Therefore, considering $FVC = FIPAR(\theta_s = 0)$, equation (7) yields (Roujean and Lacaze 2002):

$$FVC = 1 - \exp(-b \cdot G(\theta_s = 0) \cdot \Omega \cdot LAI) \quad (8)$$

In equation (8), a value of 0.5 is adopted for the leaf projection factor $G(\theta_s)$ considering spherical orientation of the foliage. In order to avoid maximum LAI values in fully vegetated areas (i.e. when FVC $\rightarrow$1) exceeding a value about 6-7, a coefficient a_0 in the range (1.04-1.07) is introduced in (8):

$$FVC = a_o \{1 - \exp(-0.5 \cdot b \cdot \Omega \cdot LAI)\} \quad (9)$$

The clumping is assumed for simplicity to be homogeneous within each vegetation cover type A cover-dependent empirical clumping index to each of the existing classes in the Global Land Cover 2000 map (GLC2000) has been adopted. The values for each biome of the GLC2000 database, correspond to the maximum values from all valid retrievals as calculated from global POLDER multiangular data for the period November 1996 to June 1997 (Chen et al. 2005). Typical clumping values are 0.68 for evergreen forest, 0.77-0.79 for deciduous forest, and 0.83-0.85 for herbaceous, shrub and cultivated areas.

The theoretical uncertainty of LAI, Err(LAI) , propagates uncertainties attached to the FVC estimate, Err(FVC), and is also associated with the uncertainties of parameters a_0, b and Ω, according to the following expression:

$$(Err(LAI))^2 = \left(\frac{Err(FVC)}{a_1(a_0 - FVC)}\right)^2 + \left(\frac{LAI \cdot Err(a_1)}{a_1}\right)^2 + \left(\frac{FVC \cdot Err(a_0)}{a_0 a_1 (a_0 - FVC)}\right)^2 \quad (10)$$

where

$$a_1 = b \cdot \Omega \quad (11)$$

Typical uncertainty values adopted for the model parameters are: Err(a_0)=0.03 and Err(a_1)=0.04.

2.5 FAPAR Algorithm description

For the retrieval of daily FAPAR from space data without any prior knowledge on the land cover, a statistical relationship general enough for global applications (Roujean and Bréon, 1995) is defined based on simulations using the homogeneous SAIL model (Verhoef, 1984). The FAPAR information is derived from the red and NIR spectral bands. The SAIL model provides the BRDF data as well as the amount of radiation absorbed by vegetation. Inputs of SAIL model are leaf inclination distribution (LIFD), LAI, leaf transmittance, leaf reflectance and soil spectral albedo. A large number of vegetation canopy radiative transfer scenarios are simulated. The diffuse fraction of incoming radiation is held constant and equal to 0.2, which represents clear sky conditions. For each scenario, red and NIR reflectances with variations of sun and view angles are obtained. Finally, the daily FAPAR is computed by integration of the instantaneous FAPAR over the day:

$$FAPAR = \frac{\int_t^{t'} APAR \; dt}{\int_t^{t'} PAR \; dt} \quad (12)$$

Where t and t' are the time for sunrise and sunset. The FAPAR was integrated over solar angles corresponding to a target located at 45ºN latitude and at the equinox.

An optimal geometry based on the criteria of linearity and minimum dispersion between NDVI and daily-integrated FAPAR is found in the solar principal plane (θ_s=45º, θ_v=60º, φ=0º). A vegetation index is thus proposed to minimize the soil reflectance effects, called RDVI (Renormalized Difference Vegetation Index) defined as follows:

$$RDVI = (NDVI \cdot DVI)^{1/2} = \frac{NIR - R}{\sqrt{NIR + R}} \quad (13)$$

Where DVI is the difference vegetation index (DVI), $(k_0)_{NIR}$ - $(k_0)_{VIS}$ (Roujean and Lacaze, 2002). Finally, the RDVI-FAPAR relationship in the optimal geometry is given in Eq. (14). In order to apply this relationship to remotely sensed data, it is needed first to be able of characterising the BRDF in order to compute the reflectance and thus the RDVI in the optimal geometry

$$FAPAR=1.81*(RDVI)_{opt} - 0.21 \quad (14)$$

Where $(RDVI)_{opt}$ refers to the RDVI computed in the optimal geometry. The reflectance in the optimal geometry (θ_s=45º, θ_v=60º, φ=0º) for each spectral channel is estimated from the Roujean et al. (1992) as follows:

$$R_{opt}(\lambda)=k_0(\lambda) - 0.240* k_1(\lambda) + 0.202* k_2(\lambda) \quad (15)$$

The theoretical FAPAR uncertainty is assessed by mathematically differentiating Eq. (13) with respect to the theoretical input error. The error of the BRDF parameters correspond with the diagonal elements of the uncertainty covariance matrix i.e. the C00, C11 and C22 fields of the BRDF error estimate (i.e. AL-Ci-CK product) for the three model parameters (SAF/LAND/MF/PUM_AL/1.6v2). Therefore, the error of the FAPAR is computed as:

$$Err(FAPAR) = 1.81 \cdot Err(RDVI) \quad (16)$$

$$Err(RDVI) = \left[Err(R(C2)) + Err(R(C1))\right] \cdot \left[\frac{1}{\sqrt{R(C1) + R(C2)}} + \frac{1}{2}\frac{\left(R(C2) - R(C1)\right)}{\left(R(C1) + R(C2)\right)^{\frac{3}{2}}}\right] \quad (17)$$

Where Err(R(Ci)) in the optimal geometry used for retrieving the FAPAR is computed as:

$$Err(R) = Err(k_0) + 0.240 \cdot Err(k_1) + 0.202 \cdot Err(k_2) \quad (18)$$

And the theoretical uncertainty of the directional error is given in the C00, C11 and C22 fields of the HDF5_LSASAF_MSG_AL-C_i-CK product.

3 Product Description

3.1 Overview

The vegetation products (VEGA) are delivered at Daily (MDFVC, MDLAI, MDFAPAR) and ten-day (MTFVC, MTLAI, MTFAPAR) time step based on the cloud-free BRDF k_0 parameter. The LSA SAF SEVIRI/MSG chain processes separately four geographical areas, described in table 3 (and depicted in figure 1) as well as in a single file covering the full SEVIRI disk. The projection and spatial resolution correspond to the characteristics of Level 1.5 MSG/SEVIRI instrument data. Information on geo-location and data distribution is available at the LSA SAF web-site: http://landsaf.ipma.pt.

Table 3. Characteristics of the LSA SAF geographical areas: Each region is defined by the corner positions relative to an MSG image of 3712 columns per 3712 lines, starting from North to South and from West to East.

Region Name	Description	Initial Column	Final Column	Initial Line	Final Line	Size in Columns	Size in Lines	Total Number of Pixels
Euro	Europe	1550	3250	50	700	1701	651	1.107.351
NAfr	Northern Africa	1240	3450	700	1850	2211	1151	2.544.861
SAfr	Southern Africa	2140	3350	1850	3040	1211	1191	1.442.301
SAme	Southern America	40	740	1460	2970	701	1511	1.059.211
MSG-Disk	Full SEVIRI disk	1	3712	1	3712	3712	3712	13.778.944

3.2 Geolocation / Rectification

The SEVIRI-based fields are generated pixel-by-pixel, maintaining the original resolution of SEVIRI level 1.5 data. These correspond to rectified images to 0º longitude, which present a typical geo-reference uncertainty of about 1/3 of a pixel. Data are kept in the native geostationary projection.

Files containing the latitude and longitude of the centre of each pixel may be downloaded from the LSA SAF website (http://landsaf.ipma.pt; under “Static Data and Tools”):

Longitude

HDF5_LSASAF_MSG_LON_Euro_4bytesPrecision.bz2
HDF5_LSASAF_MSG_LON_NAfr_4bytesPrecision.bz2
HDF5_LSASAF_MSG_LON_SAfr_4bytesPrecision.bz2

HDF5_LSASAF_MSG_LON_SAme_4bytesPrecision.bz2
HDF5_LSASAF_MSG_LON_MSG-Disk.bz2

Latitude

HDF5_LSASAF_MSG_LAT_Euro_4bytesPrecision.bz2
HDF5_LSASAF_MSG_LAT_NAfr_4bytesPrecision.bz2
HDF5_LSASAF_MSG_LAT_SAfr_4bytesPrecision.bz2
HDF5_LSASAF_MSG_LAT_SAme_4bytesPrecision.bz2
HDF5_LSASAF_MSG_LAT_MSG-Disk.bz2

Alternatively, since the data are in the native geostationary projection, centred at 0º longitude and with a sampling distance of 3 km at the sub-satellite point, the latitude and longitude of any pixel may be easily estimated. Given the pixel column number, *ncol* (where *ncol*=1 correspond to the westernmost column of the file), and line number, *nlin* (where *nlin*=1 correspond to the northernmost line), the coordinates of the pixel may be estimated as follows:

$$lon = arctg\left(\frac{s_2}{s_1}\right) + sub\_lon$$ longitude (deg) of pixel centre

$$lat = arctg\left(p_2 \cdot \frac{s_3}{s_{xy}}\right);$$ latitude (deg) of pixel centre

where

sub_lon is the sub-satellite point ($sub\_lon = 0$)

and

$$s_1 = p_1 - s_n \cdot \cos x \cdot \cos y$$

$$s_2 = s_n \cdot \sin x \cdot \cos y$$

$$s_3 = -s_n \cdot \sin y$$

$$s_{xy} = \sqrt{s_1^2 + s_2^2}$$

$$s_d = \sqrt{(p_1 \cdot \cos x \cdot \cos y)^2 - (\cos^2 y + p_2 \cdot \sin^2 y) \cdot p_3}$$

$$s_n = \frac{p_1 \cdot \cos x \cdot \cos y - s_d}{\cos^2 y + p_2 \cdot \sin^2 y}$$

where

$$x = \frac{ncol - COFF}{2^{-16} \cdot CFAC}$$ (in Degrees)

$$y = \frac{nlin - LOFF}{2^{-16} \cdot LFAC}$$ (in Degrees)

$p_1 = 42164$

$p_2 = 1.006803$

$p_3 = 1737121856$

$CFAC = 13642337$

LFAC=13642337

The CFAC and LFAC coefficients are column and line scaling factors which depend on the specific segmentation approach of the input SEVIRI data. Finally, COFF and LOFF are coefficients depending on the location of the each LSA SAF geographical area within the Meteosat disk. These are included in the file metadata (HDF5 attributes; Annex C), and correspond to one set of the values detailed below per SEVIRI/MSG area (table 4):

Table 4. Maximum values for number of columns (ncol) and lines (nlin), for each LSA SAF geographical area, and the respective COFF and LOFF coefficients needed to geo-locate the data.

Region Name	Description	Maximum *ncol*	Maximum *nlin*	COFF	LOFF
Euro	Europe	1701	651	308	1808
NAfr	Northern Africa	2211	1151	618	1158
SAfr	Southern Africa	1211	1191	-282	8
SAme	Southern America	701	1511	1818	398
Disk	Full Disk	3712	3712	1857	1857

3.3 File names and formats

At each execution the VEGA algorithm generates six output files with the following name convention:

daily products:

- **HDF5_LSASAF_MSG_FVC_Region_YYYYMMDD0000.bz2**
- **HDF5_LSASAF_MSG_LAI_Region_YYYYMMDD0000.bz2**
- **HDF5_LSASAF_MSG_FAPAR_Region_YYYYMMDD0000.bz2**

10-day products:

- **HDF5_LSASAF_MSG_FVC-D10_Region_YYYYMMDD0000.bz2**
- **HDF5_LSASAF_MSG_LAI-D10_Region_YYYYMMDD0000.bz2**
- **HDF5_LSASAF_MSG_FAPAR-D10_Region_YYYYMMDD0000.bz2**

where Region, YYYY, MM, and DD denote the region name, year, month and day of data acquisition, respectively. The LSA SAF products are provided in the HDF5 format developed by

the NCSA (National Center for Supercomputing Applications) at the University of Illinois. A comprehensive description is available at http://hdf.ncsa.uiuc.edu/.
Libraries for handling HDF5-files in Fortran and C are available at ftp://ftp.ncsa.uiuc.edu/HDF/HDF5/hdf5-1.6.2/. A user friendly graphical interface to open and view HDF5-files can be downloaded from http://hdf.ncsa.uiuc.edu/hdf-java-html/hdfview/. The HDF5-format permits the definition of a set of attributes for providing relevant information. Each LSA SAF product file includes the general attributes listed in Table 10 of Annex C. Within the HDF5-files the information is organised in the form of separate datasets. For each dataset a set of additional attributes is available.

3.4 Product Content

The FVC, LAI and FAPAR products contain 3 datasets each, comprising the following fields:

- a vegetation field
- an error estimate field
- a quality control information field.

The data is coded in HDF5 format. The HDF5 files in LSA SAF system have the following structure:

- A common set of attributes for all kind of data, containing general information about the data (including metadata compliant with U-MARF requirements);
- A dataset for the parameter values;
- Additional datasets for metadata (e.g., quality flags).

The products and their respective error estimates are produced using the HDF5 signed 16-bit integer variable. The values are stored in their digital form with a scale-factor (gain), which is applied to transform the stored values to their biophysical counterparts for analysis. The quality control variables are 8-bit unsigned integer measures without a gain or offset. Tables 5, 6 and 7 show the contents of the FVC, LAI and FAPAR products (either for daily or 10-days products), respectively. Detailed information is given in Annex C. Note that the range for the respective product errors refers to the confidence intervals for valid pixels, although higher errors can be also found in a few areas (less than 1% of retrieved pixels). Beyond these uncertainty limits (0.2 for FVC and FAPAR, and 1.5 for LAI) estimations may be regarded as unreliable and its use should be restricted.

Table 5. Content of the FVC product.

Parameter	Dataset name	Range	Variable Type	Scale Factor
Fractional vegetation cover	FVC	[0, 1]	2-Byte Signed Integer	10000
Product error	FVC_err	[0, 0.2]	2-Byte Signed Integer	10000
Quality Flag	FVC_QF	[0,255]	1-Byte Unsigned Integer	na

Table 6. Content of the LAI product.

Parameter	Dataset name	Range	Variable Type	Scale Factor
Leaf area index	LAI	[0, 7]	2-Byte Signed Integer	1000
Product error	LAI_err	[0, 1.5]	2-Byte Signed Integer	1000
Quality Flag	LAI_QF	[0,255]	1-Byte Unsigned Integer	na

Table 7. Content of the FAPAR product.

Parameter	Dataset name	Range	Variable Type	Scale Factor
Fraction of Absorbed Photosynthetic Active Radiation	FAPAR	[0, 1]	2-Byte Signed Integer	10000
Product error	FAPAR_err	[0, 0.2]	2-Byte Signed Integer	10000
Quality Flag	FAPAR_QF	[0,255]	1-Byte Unsigned Integer	na

An example of the LSA SAF VEGA (FVC, LAI and FAPAR) v3.0 daily products is shown in Figure 3. The outputs present practically no missing data except for areas which are usually covered by snow or frequent cloud cover. Large uncertainties are generally found in areas where the BRDF reliability is poor. The higher values of the different vegetation fields are found in the Amazon Basin and Central Africa forest. The products display large spatial variations representing the main vegetation gradients. In the African continent, the products are equal to 0 over the Sahara desert and increase over the Sahel, reaching the highest values over the equatorial evergreen forest and a gradually decrease through the intermediate woodlands and shrublands to the Namibian desert. Detailed information about the quality of the products, including the assessment of the spatial and temporal consistency are given in a related document (SAF/LAND/UV/VEGA_VR/2.1-5).

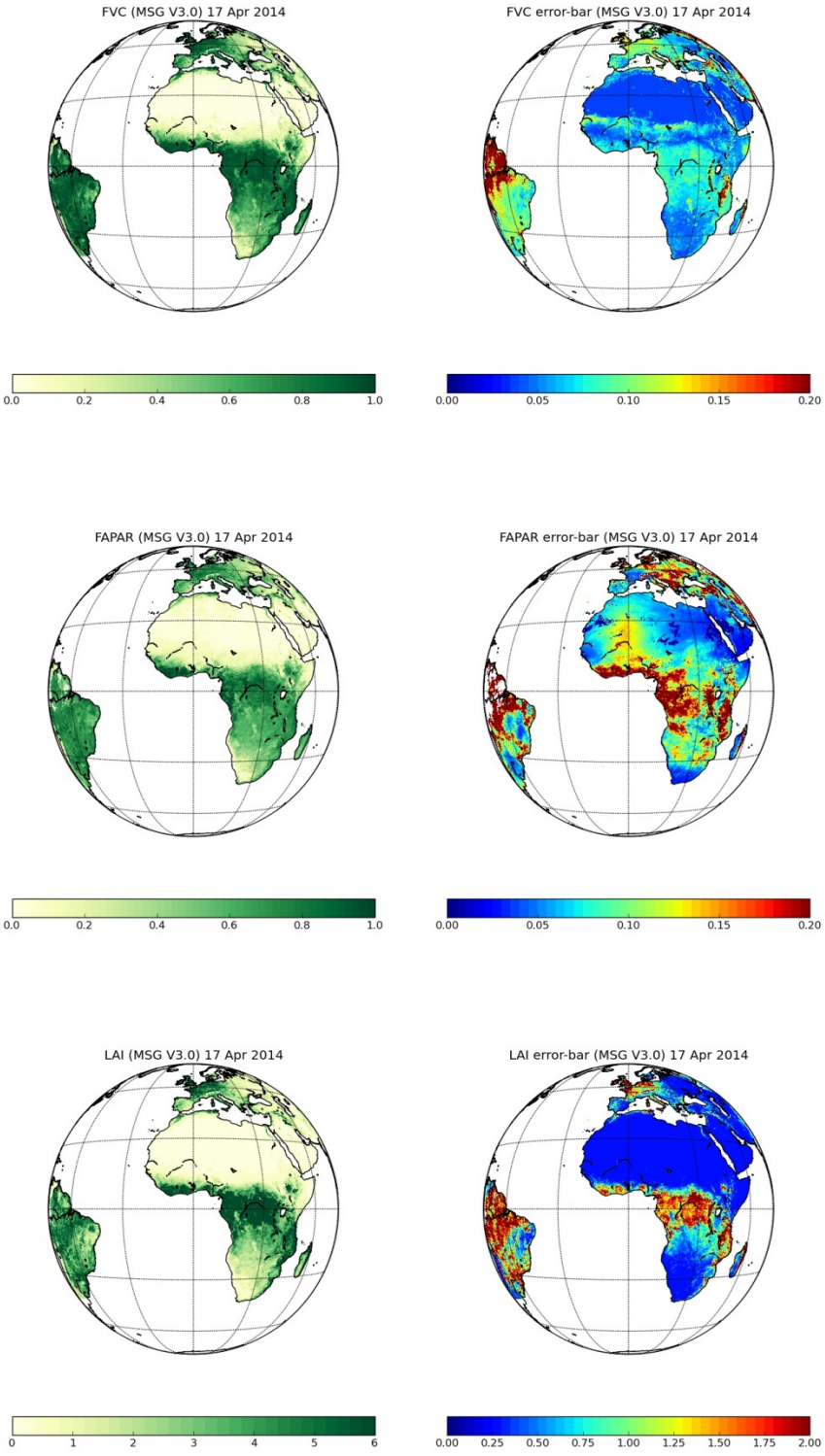

Figure 3. MSG Daily LAI (top), FVC (middle) and FAPAR (bottom) LSA SAF VEGA (version v3.0) product composition of the four LSA SAF geographical areas corresponding to the 17th of April 2014: products (left panels) and their respective error estimates (right panels).

The users are advised to pay attention to the quality flag files accompanying the products. Quality control measures are currently produced at the pixel level and represented by the error estimate and the quality flag separate data layers in the HDF5 file whose pixel values correspond to specific quality scoring schemes. Considerable attention has been paid to implement a set of quality control protocols that help users match data sets to their applications. The details of the quality flag information for FVC, LAI and FAPAR are summarized in Tables 8 and 9. In particular, table 9 lists the main identified problems in the VEGA products and provides the associated empirical thresholds used to blind problematic areas.

Table 8. VEGA products Q-Flag information. The default Missing Value for the product fields is -10. The associated error estimate fields for unprocessed pixels take different negative values, depending on the identified problem (default Missing Value =-10).

Bit		Binary Code	Description	Products are processed
Bits 0-1	Land Sea Mask(*)	00	Ocean	No
		01	Land	Yes
		10	Space (Outside of MSG disk)	No
		11	Continental water	No (errors set to -20)
Bit 2	MSG(*)	0	No MSG Observations	Yes
		1	Including MSG Observations	Yes
Bit 3	Traces of inland water	0	No	Yes
		1	High Probability	Yes
Bit 4	Traces of snow cover	0	No	Yes
		1	High Probability	No (errors set to -31)
Bit 5	Snow(*)	0	No Snow	Yes
		1	Snow	No (errors set to -30)
Bit 6	Unrealistic Input ranges	0	Reliable	Yes
		1	Unreliable	No (errors set to -40)
Bit 7	Failure(*)	0	Input Normally Processed	Yes
		1	Input Algorithm Failed	No

(*) This information is reported from the BRDF product quality flag to the VEGA product quality flag.

Table 9. Main identified problems in the VEGA products and empirical thresholds used to blind problematic areas. Note that although the Missing Value for the product fields is unique (-10), associated error estimate fields for unprocessed pixels take different negative values, depending on the identified problem (default Missing Value =-10).

Identified problem	Condition	Products are processed
Traces of snow	$k_o(\lambda_1) - k_o(\lambda_3) > 0$ *or* $k_o(\lambda_1) > k_{o,\max}(\lambda_1) + 0.06$ *or* $(k_o(\lambda_1) > k_{o,\max}(\lambda_1) + 0.02$ *and* $k_o(\lambda_3) < k_{o,\min}(\lambda_3))$	No (bit 4 set to 1, Errors set to -31)
Unrealistic input ranges (*)	$k_o(\lambda_2) < 0.03$ or $k_o(\lambda_3) < 0.03$ or $\sum_{i=1}^{3} k_o(\lambda_i) < 0.03$	No (bit 6 set to 1, errors set to -40)
Traces of inland water(**)	$\sum_{i=1}^{3} k_o(\lambda_i) < 0.09$	Yes (bit 3 set to 1)
Large k_0 errors	$\frac{1}{3}\sum_{i=1}^{3} \mathrm{Err}(k_o(\lambda_i)) < 0.10$	No (Errors set to -15)
Large k_2 errors	$\mathrm{Err}(k_2(\lambda_1)) > 0.25$ or $\mathrm{Err}(k_2(\lambda_2)) > 0.25$	Yes (FVC, LAI) No (FAPAR) FAPAR_err=-50
Large BRDF errors in optimal geometry	$Err(R_{opt}(\lambda_1)) > 1.0$ *or* $Err(R_{opt}(\lambda_2) > 1.0$	Yes (FVC, LAI) No (FAPAR) FAPAR_err=-50
Unrealistic input in optimal geometry	$R_{opt}(\lambda_2) < 0.03$ *or* $(R_{opt}(\lambda_1) + R_{opt}(\lambda_2)) < 0.06$	Yes (FVC,LAI) No (FAPAR) FAPAR_err=-40
Out of FAPAR physical range (***)	FAPAR >1	Yes (FVC,LAI) No (FAPAR) FAPAR_err=-60 FAPAR=-60

(*) The BRDF algorithm produces values out of the physical ranges in a few areas (i.e. less than 1% of land surface). Typical examples correspond to high reflectance values (e.g. for NIR reflectance at high latitudes) or negative values (e.g., for red reflectance at high view zenith angle geometries). Very dark reflectance pixels are discarded, whereas abnormally bright pixels are set to a reflectance to a maximum value (typically 0.70, 0.80 and 0.90 for the red, NIR and MIR bands, respectively).

(**) These areas should be taken with special caution by the user, since the reliability of the product may be low. This problem affects, however, to less than 0.5% of land surface pixels and is mainly located in the SAme geographical zone.

(***) FAPAR retrieval values out of maximum physical range are blinded (this problem affects only to less than 1% of land pixels). For values below 0 the FAPAR product is set to 0; this affects only to desert areas (eg. Sahara).

3.5 Quality control

Figures 4 and 5 show the spatial distribution of the mean FVC, LAI and FAPAR uncertainty along the year 2014. Green areas correspond with regions where the mean value of the product error along the year is below 0.05 (for FVC and FAPAR) or below 0.5 (for LAI). These regions are thus considered as consolidated areas with optimal quality. In cyan colour, areas with medium quality are showed (uncertainty between 0.05 and 0.10 for FVC and FAPAR and between 0.5 and 1.0 for LAI). The products are reliable in these regions although they could present some problems depending on the period. The areas in orange correspond to those regions with low quality, the mean uncertainty along the year is typically between 0.10 and 0.15 (for FVC and FAPAR) and between 1.0 and 1.5 (for LAI). Finally, red colour corresponds to generally unusable areas, i.e. with errors higher than 0.15 (for FVC and FAPAR) or higher than 1.5 (for LAI). These areas correspond mainly to regions with large view zenith angles (e.g., North of Europe, South America), with frequent snow cover as in Europe during wintertime or with persistent cloud coverage as in western Africa.

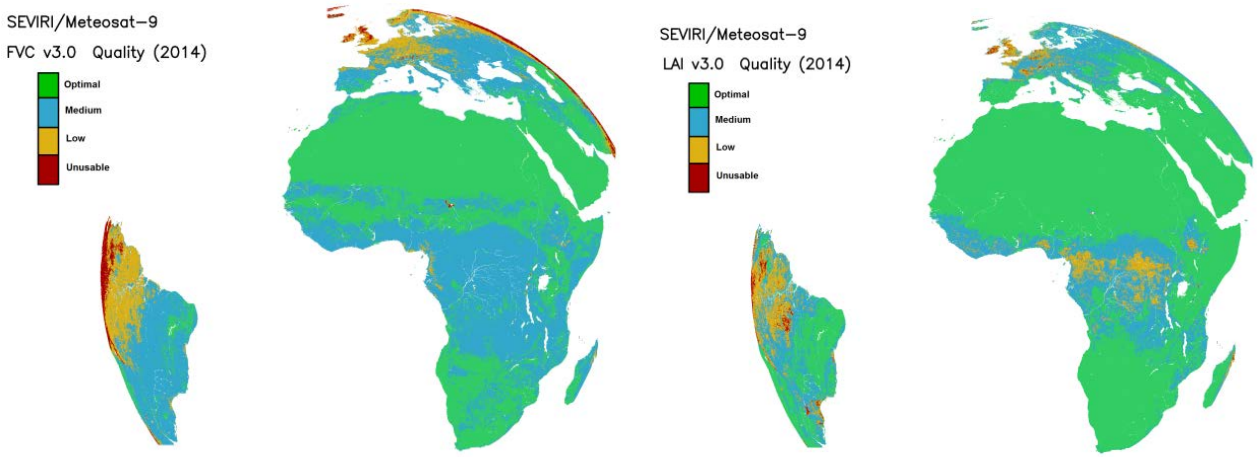

Figure 4. Quality of the MSG Daily FVC and LAI products as a function of the mean values of its theoretical uncertainty along the year 2014 (see text for details).

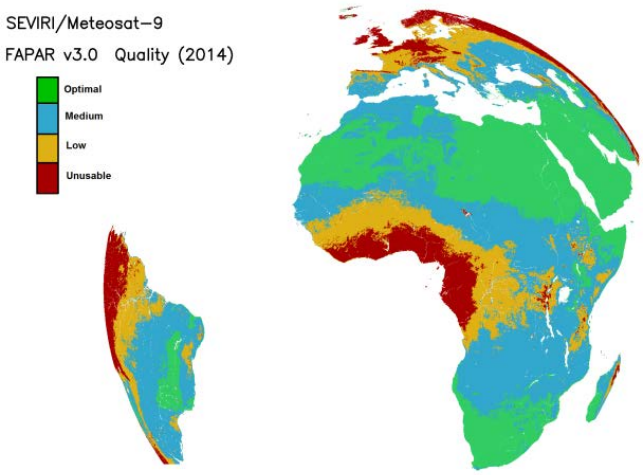

Figure 5. Quality of the MSG Daily FAPAR product as a function of the mean values of its theoretical uncertainty along the year 2014 (see text for details).

The seasonal variations in the quality and coverage of the LSA SAF MDFVC product during year 2014 are depicted in Figure 6. Clearly, the best performance of the FVC corresponds to the NAfr and SAfr continental zones, with optimal quality retrievals in about 80% of the regions and a negligible percentage of poor quality or unprocessed pixels. A good performance is also found over Europe from April through September, although the quality of the product rapidly deteriorates during late autumn and winter. The SAme continental zone presents generally the worst performances due to decreased accuracy and a larger percentage of unprocessed pixels. The performance of MDLAI and MDFAPAR products is similar, although with slightly lower rates of high quality values.

Figure 6. Monthly fraction of valid inland pixels for LSA SAF MSG Daily FVC product during year 2014 over the four SEVIRI geographical regions. Percentages are classified according to three main levels of accuracy: optimal (Err(FVC)<0.05); medium to low (0.05<Err(FVC)<0.15); poor Err(FVC)>0.15.

3.6 Changes from v2.1 to v3.0

Two important improvement was made in the current (v3.0) version

i) To more reliably determine the probability of soil/vegetation models by considering simultaneously the dates of maximum/minimum canopy closure (i.e the vegetated/devegetated k_0 images) in the estimation $p(M_K|\mathbf{r})$, i.e. the membership of model M_K given pixel data $\mathbf{r}$,. For example, a devegetated image was obtained corresponding to periods that do not have significant vegetation cover (e.g. dry season and harvested crops in some areas) allowing thus improve identyfing the spectral characteristics of underlaying soil background. We refer for details to SAF/LAND/MF/ATBD_ETAL/1.3.

ii) Improve the condition to identify residual snow, which may cause important changes in surface reflectance during consecutive days, and important biases in the resulting FVC/LAI estimates (FAPAR is less affected by this problem because it does not use as input the SEVIRI channel 3). In order to illustrate the impact of these errors over Europe during wintertime, several joint probability density plots between two daily LSA SAF FVC estimates with an 8-day offset are depicted in Figure 7. Different threshold values *Th* (see Eq. 22) are used to filter out the observations most likely affected by snow contamination. In this example, the condition *Th*=0 makes a credible job to remove a significant part of the

undesired scattering (eg. RMS differences drops to an acceptable value of 0.029) while retaining 90.3% of the pixels.

iii)

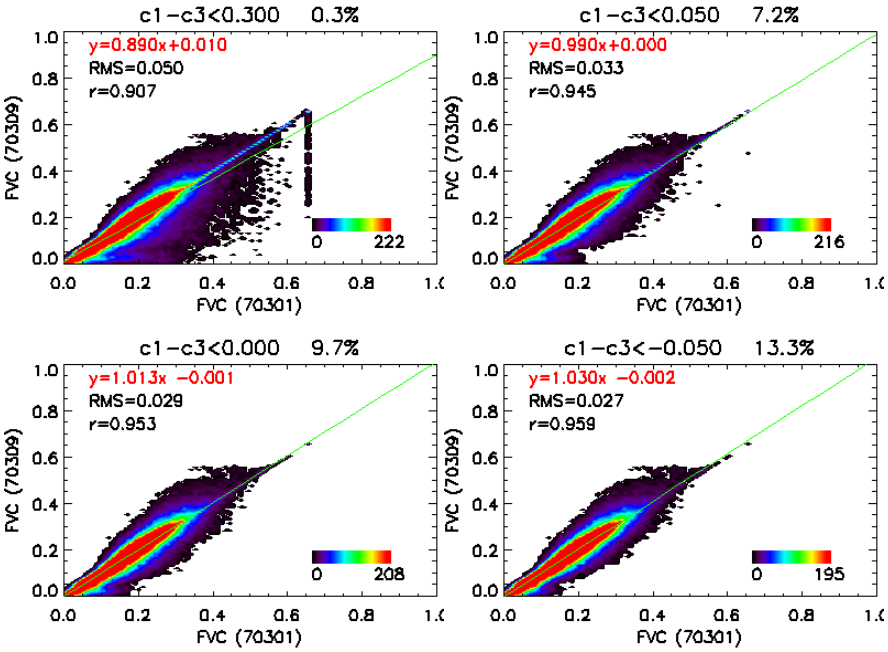

Figure 7. Scatter-plots of FVC retrievals for two close dates, 1th March and 9th March, as a function of the threshold criterion used to mask snow-affected areas. Note that Th=0 correspond to the left bottom graph. 70301 and 70309 refer to day of production in format (ymmdd), with year=2014.

In the v2.0 version problematic areas were processed and, therefore, users are advised to use associated quality information to discard unusable estimations, see Table 8. As a consequence of snow effects, a non-reliable pattern of FVC and LAI v2.0 was found during winter over numerous regions in Europe. One major difference of the VEGA v2.1 and the current VEGA v3.0 versions, compared with the v2.0 one is that areas with low quality inputs are not processed. In VEGA version 2.1 an empirical criterion was used to identify the presence of residual snow over Euro region, by combining the SEVIRI channels 1 (0.6 μm) and 3 (1.6 μm):

$$k_o(\lambda_1) - k_o(\lambda_3) > Th \tag{22}$$

where *Th* represents a prescribed threshold, which was set to 0.0.

Nevertheless, in VEGA version 3.0 two additional conditions have been introduced to more reliably blind contaminated pixels.

(i) When Equation 22 holds, setting *Th*=0.

(ii) when the reflectance in channel 1 ($k_o(\lambda_1)$) is abnormally bright, exceeding the reflectance of the devegetated pixel, namely $k_{o,\max}(\lambda_1)$, in a threshold value of Th_1=0.06;

(iii) when $k_o(\lambda_1)$ exceeds $k_{o,\max}(\lambda_1)$ in Th_2=0.02 and furthermore the reflectance in channel 3 is small (less than the that of a devegetated pixel, $k_{o,\min}(\lambda_3)$).

Thus in the current (v3.0) snow pixels (unprocessed) are identified as follows:

$$\begin{aligned} & k_o(\lambda_1) - k_o(\lambda_3) > Th \\ \textit{or} \quad & k_o(\lambda_1) > k_{o,\max}(\lambda_1) + Th_1 \\ \textit{or} \quad & (k_o(\lambda_1) > k_{o,\max}(\lambda_1) + Th_2 \quad \textit{and} \quad k_o(\lambda_3) < k_{o,\min}(\lambda_3)) \end{aligned} \tag{23}$$

$k_{o,\max}(\lambda_1)$ and $k_{o,\min}(\lambda_3)$ refer to the values of the k_o devegetated image in red and MIR bands, respectively, which was constructed by compositing the k_o values corresponding to the minimum FVC.

The use of a more accurate condition for masking unreliable inputs (e.g. presenting unidentified residual snow) improved the reliability of the VEGA v3.0 estimates (mainly for FVC and LAI), as illustrated in Figure 8. Some artefacts in FVC profiles during winter in some European areas due to unidentified snow contamination are removed in the current (v3.0) version. Further details are provided in Figure 9, which compares both versions of FVC (v2.1 and v3.0)) in a day with high snow coverage in Europe. FVC v3.0 realistically identifies as snow some areas adjacent to flagged by snow, particularly in central and southwestern areas, leaving thus unprocessed pixels with positively biased FVC values due to snow contamination. We can also observe that even under suboptimal conditions (wintertime in Europe) both FVC versions (v2.1 and v3.0) are consistent. Existing differences between FVC versions are related with changes in the v3.0 algorithm, which provides a more accurate identification of the vegetation and soil components, improving notably the consistency with Copernicus Global Land products based on SPOT/VEGETATION observations (García-Haro et al. 2016).

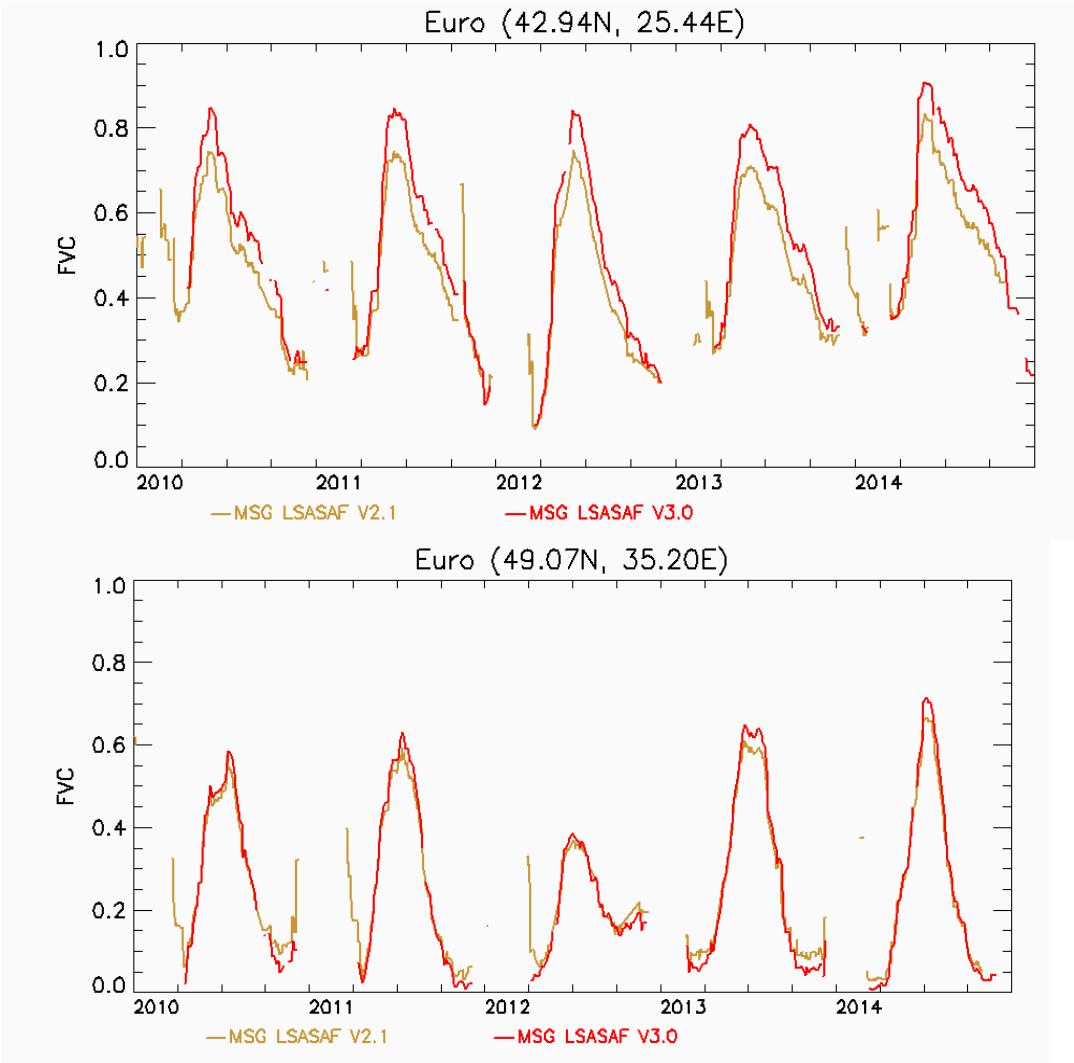

Figure 8. Time profiles of FVC (versions v2.1 and v3.0) for two areas in Europe, illustrating the improvement in reliability of the new condition to blind snow contaminated pixels.

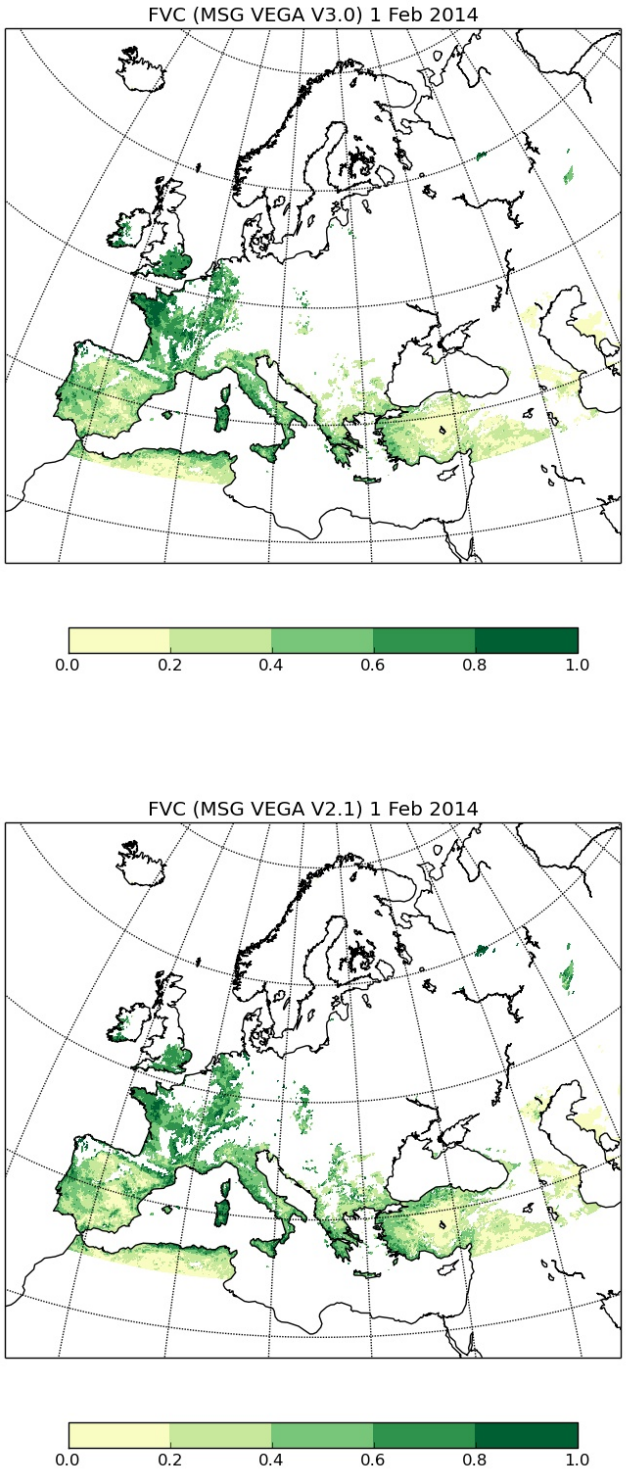

Figure 9. Comparison of FVC product (versions v2.1 and v3.0) over Europe for the 1st of February 2014.

3.7 Summary of Product Characteristics

3.7.1 FVC

Product Name:	Fractional Vegetation Cover (FVC)
Product Code:	MDFVC (LSA-401), MTFVC (LSA-402)
Product Level:	Level 3

Product Parameters:

Coverage:	MSG full disk (Continental pixels over land)
Packaging:	Europe, N_Africa, S_Africa, S_America, MSG-Disk
Sampling:	pixel by pixel basis
Spatial Resolution:	MSG full resolution (3km×3km at nadir)
Projection:	SEVIRI instrument projection
Units:	unitless
Range:	0 - 1
Target accuracy:	Max [0.075, 15%]
Format:	16 bits signed integer (FVC and error estimates)
	8 bits (quality flag)
Frequency of Generation:	daily and 10-day
Size of Product Files:	FVC Euro (uncompressed): 5.42 Mb
	FVC N_Africa (uncompressed): 12.44 Mb
	FVC S_Africa (uncompressed): 7.05 Mb
	FVC S_America (uncompressed): 5.18 Mb
	FVC MSG-Disk (uncompressed): 67.292 Mb

Additional Information:

Identification of bands used in algorithm:

BRDF k0 VIS 0.6

BRDF k0 NIR 0.8

BRDF k0 MIR 1.6

Assumptions on input data: Radiometric, Geometric and atmospheric corrections

3.7.2 LAI

Product Name:	Leaf Area Index (LAI)
Product Code:	MDLAI (LSA-404), MTLAI (LSA-405)
Product Level:	Level 3

Product Parameters:

Coverage:	MSG full disk (Continental pixels over land)
Packaging:	Europe, N_Africa, S_Africa, S_America, MSG-Disk
Sampling:	pixel by pixel basis
Spatial Resolution:	MSG full resolution (3km×3km at nadir)
Projection:	SEVIRI instrument projection
Units:	$m^2 \cdot m^{-2}$
Range:	0 - 7
Target accuracy:	Max [0.5, 20%]
Format:	16 bits signed integer (LAI and error estimates)
	8 bits (quality flag)
Frequency of Generation:	daily and 10-day
Size of Product Files:	LAI Euro (uncompressed): 5.42 Mb
	LAI N_Africa (uncompressed): 12.44 Mb
	LAI S_Africa (uncompressed): 7.05 Mb
	LAI S_America (uncompressed): 5.18 Mb
	LAI MSG-Disk (uncompressed): 67.292 Mb

Additional Information:

Identification of bands used in algorithm:	VEGA FVC
Assumptions on input data:	Radiometric, Geometric and atmospheric corrections
Identification of ancillary and auxiliary data:	Land Cover (GLC2000), Clumping Index.

3.7.3 FAPAR

Product Name:	Fraction of Absorbed Photosynthetically Active Radiation (FAPAR)
Product Code:	LSA-407 (MDFAPAR), LSA-408 (MTFAPAR)
Product Level:	Level 3

Product Parameters:

Coverage:	MSG full disk (Continental pixels over land)
Packaging:	Europe, N_Africa, S_Africa, S_America, MSG-Disk
Sampling:	pixel by pixel basis
Spatial Resolution:	MSG full resolution (3km×3km at nadir)
Projection:	SEVIRI instrument projection
Units:	unitless
Range:	0 - 1
Target accuracy:	Max [0.075, 15%]
Format:	16 bits signed integer (FAPAR and error estimates)
	8 bits (quality flag)
Frequency of Generation:	daily and 10-day
Size of Product Files:	FAPAR Euro (uncompressed): 5.42 Mb
	FAPAR N_Africa (uncompressed): 12.44 Mb
	FAPAR S_Africa (uncompressed): 7.05 Mb
	FAPAR S_America (uncompressed): 5.18 Mb
	FAPAR MSG-Disk (uncompressed): 67.292 Mb

Additional Information:

Identification of bands used in algorithm:

BRDF k0 VIS 0.6
BRDF k0 NIR 0.8
BRDF k1 VIS 0.6
BRDF k1 NIR 0.8
BRDF k2 VIS 0.6
BRDF k2 NIR 0.8

Assumptions on input data: Radiometric, Geometric and atmospheric corrections

Identification of ancillary and auxiliary data: no used.

4 Validation and Quality Control

4.1 Validation

The adopted strategy for validation of VEGA products (FVC, LAI and FAPAR) consists on three main steps: 1) inter-comparison with other satellite derived vegetation products (particularly, MODIS, MERIS and VGT); 2) comparison with in situ measurements; 3) evaluation of errors in the main variables used as input for VEGA algorithm and assessment of the impact on VEGA products. Up to now, several versions of the validation reports have been issued:

- SAF/LAND/IM/VR/1.5 (January 2006) evaluates MSG Daily FVC and LAI products (version v1.2)
- SAF/LAND/UV/VEGA_VR/2.0 (January 2007) evaluates MSG Daily FVC, LAI and FAPAR products (version v2.0)
- SAF/LAND/UV/VEGA_VR/2.1 (January 2008) evaluates MSG Daily FVC, LAI and FAPAR products (version v2.1)
- SAF/LAND/UV/VEGA_VR/2.1-4 (December 2011) evaluates MSG Daily FVC, LAI and FAPAR products and MSG Ten-days FVC, LAI and FAPAR products.
- SAF/LAND/UV/VEGA_VR/2.1-4 (November 2013) updated version including inter-comparisons with Copernicus Global Land products.
- SAF/LAND/UV/VR_VEGA/2.1-5 (November 2015) updated version including the evaluation of the daily FVC and LAI products (version 3.0), primarily based on the intercomparison with Copernicus Global Land products.
- SAF/LAND/UV/VR_VEGA_MSG/3.0 (July 2017) updated version including the evaluation of the daily Climate Data Record (CDR) of 10-day reprocessed products since 2004.

Results obtained in these validation exercises clearly indicate that VEGA products should provide an accepted added-value with regard to similar existing products, in particular the products offer important improvements on the spatial coverage and temporal continuity.

The intercomparison with Global Land Copernicus products revealed a positive bias of FVC and LAI version (v2.1) in certain regions (South America and sparsely vegetated regions in Africa). The current (v3.0) version has important reduction of this bias, and a remarkably good performance over all regions. For example for FVC retrievals in Africa, the percentage of residuals within the optimal consistency of FVC (<0.05) changes from 57% to 74%. We refer for details to SAF/LAND/UV/VEGA_VR/2.1-5.

Automatic Quality Control (QC) is performed on each VEGA (FVC, LAI and FAPAR) product and the quality information is provided on a pixel basis. As shown in Tables 8 and 9, VEGA QC contains general information about input data quality, specific information related with the limits of application and information about confidence level of VEGA products. In particular, the product

error is the most general quality indicator operationally delivered by the algorithm. The statistical confidence intervals take into account outcome of theoretical studies and the analysis of temporal profiles.

The 10-day VEGA products, generated from MTAL composite, corresponds to a climate data record (CDR) product (National Research Council, 2004). Because of its temporal characteristics, it could be suitable for a community of users, which require an observation representative of a 30-day period. Note that many users find daily products to be too much information and prefer the 10-day composites (as condensed form). Several similar products (e.g. COPERNICUS) are also disseminated at a frequency of 10 days. Temporal profiles of the 10-day VEGA product were verified through a comparison with the VEGA daily product. Detailed information is given in a related document (SAF/LAND/UV/VR_VEGA/2.1-5). A very good agreement was found for the three VEGA products. The higher smoothness of the temporal profiles achieved with the 10-day products is relevant in the case the FAPAR product, i.e. the noisy profiles observed for some locations in the MDFAPAR product becomes smoothed in the MTFAPAR. In figure 10 we can observe a good consistency between the 10-day and the daily FVC and LAI products for the current (v3.0) version (note that the FAPAR product was not modified in version 3.0).

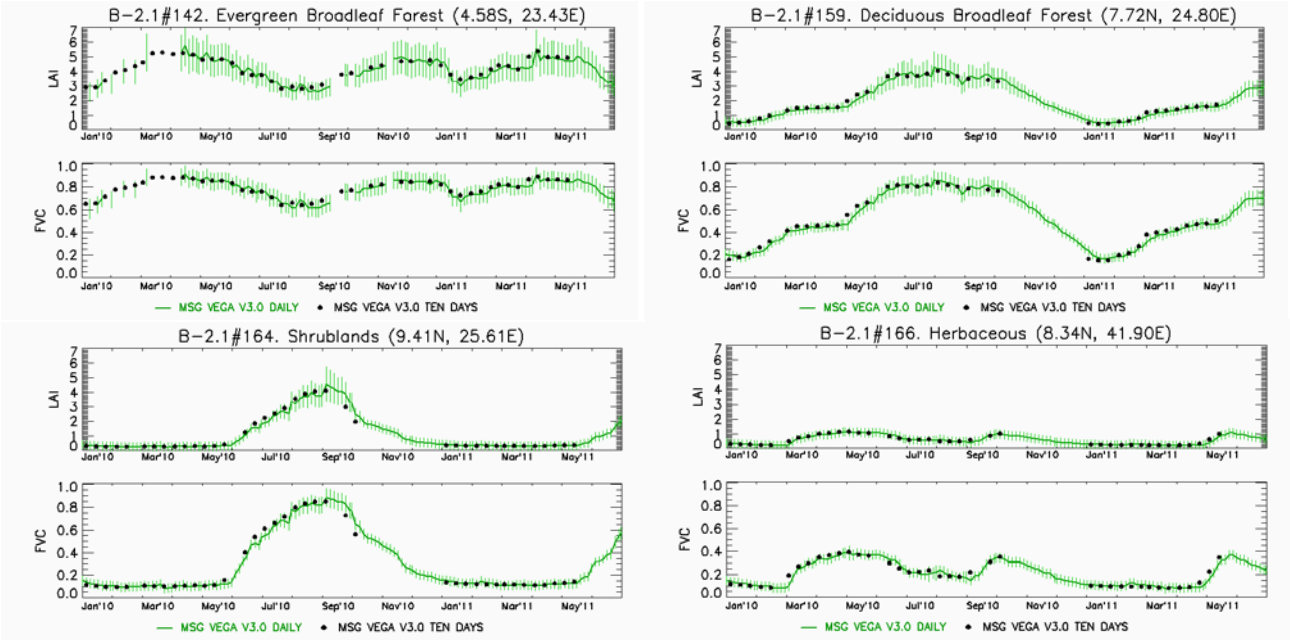

Figure 4. Time series of VEGA v3.0 daily and ten-day products at four representative BELMANIP sites. Missing data correspond either to unavailable observations or to different conditions for which the output were not generated.

A good agreement was found with equivalent products derived in the Copernicus Global Land Service (i.e. GEOV1) (see table 10). The validation results of the MSG VEGA CDR products is provided in a related document (SAF/LAND/UV/VR_VEGA_MSG/3.0), showing overall good

results, with good spatial and temporal consistency as compared to validated satellite products. Most of the criteria evaluated shows in overall positive results. No presence of artefacts (which were present in previous versions) has been found in the CDR. Most of the criteria evaluated shows in overall positive results. It is noticeable the good inter-annual precision of the products and the stability of the time series.

Table 10. Compliance matrix of MSG VEGA CDR (MTLAI-R, MTFVC-R, MTFAPAR-R) products against ground references over limited number of samples and against operational satellite products over a global network of validation sites and two year period (2015-2016). N stands for the number of samples.

MSG VEGA CDR	Ground References N=15			Copernicus GEOV1/VGT (N >26900)			NASA MODIS C5 (N > 23900)	
	LAI	FAPAR	FVC	LAI	FAPAR	FVC	LAI	FAPAR
% Optimal	61.5	No data	53.3	24.8	41.1	60.1	18.0	25.3
% Target	84.6	No data	60.0	76.1	50.8	73.4	59.0	40.3
% Threshold	92.3	No data	80.0	83.5	58.8	83.5	68.6	56.0

5 Known issues and limitations

The new version (v3.0) has been developed improving the description of soil and vegetating components in the FVC and LAI algorithms. This has contributed to reduce the observed bias and enhance the consistency with similar products derived in the Copernicus Global Land Service.

The spatial and temporal coverage of the LSA SAF vegetation product is mainly limited by large input BRDF errors at high view zenith angles and changing conditions of the surface during the compositing period (e.g. residual snow) over Europe during wintertime. The accuracy of the BRDF estimates will be dependent on intrinsic limitations of the BRDF model. Some of the approximations made in the derivation of Roujean BRDF model lose their validity when applied on dense vegetated surfaces (forests) with a large range of sun angles (Roujean et al., 1992), which partly explain large theoretical errors of BRDF often found for surfaces located at high latitudes and in the winter period

Large product errors correspond with unreliable estimations typically derived under sub-optimal BRDF sampling (e.g. South America, wintertime in Europe or areas with persistent cloud cover). Further, the algorithm does not process very dark spectra, because they tend to be noisy. Detailed information about the scientific quality of the products is given in a related document (SAF/LAND/UV/VEGA_VR/3.1).

Algorithms to retrieve vegetation parameters suffer from some loss of sensitivity since reflectance approaches saturation asymptotically under conditions of moderate-to-high green aboveground

biomass. In these conditions, the small variations in the spectral reflectance levels cannot be related accurately to the actual LAI of the canopy. The use of the SEVIRI channel 3 in the algorithm to retrieve FVC/LAI provides potentially a higher level of information on canopy structure and optical properties of its elements as compared to the simple use of the classical red and near infrared bands implemented in most other retrieval approaches. However, this makes the algorithm more sensitive to traces of snow, ice and other environmental factors (1.6 μm is a strong absorption band for snow), and may cause an important overestimation of FVC and LAI retrievals.

In closed forest canopies the multi-layer structure is responsible of a high amount of shadow, thereby reducing reflected radiant flux from the surface decreases and decreasing the signal-to-noise decreases. Consequently, higher estimating errors of FVC are usually found over dark surfaces such as needle-leaf forests in Europe (e.g. Landes forest, France) and the tropical evergreen forests in Central Africa and South America. Definitions of satellite products such as LAI are based on simplifying assumptions. Woody fraction is never accounted and leaf clumping is usually only partly accounted. One limitation of SEVIRI LAI products is that clumping effects are incorporated using a biome map (i.e. the GLC2000 global land cover) to select the vegetation types present in the SEVIRI pixel and clumping values extracted from the literature (Chen et al., 2005). Another source of uncertainty is inherent to errors in the identification of soil and vegetation components provided the variability of the mixed pixel at the SEVIRI scale.

The algorithm to retrieve VEGA products over land surfaces requires ideally free of snow and ice cover observations. Thus FVC, LAI and FAPAR products are derived from observations declared as snow-free over land. Since snow events in previous days, though influencing the signal, may be unidentified by the AL2 product, a traces of snow condition was thus necessary for masking unreliable inputs. However, spurious areas with unidentified residual snow may still be present. A typical assumption is that sudden drops in a biophysical parameter profiles are mainly related to incomplete atmospheric correction, poor illumination conditions, extreme solar zenith angles, snow and cloud contamination.

The BRDF product time series may still contain spurious variability on short time scales, which may be caused by atmospheric effects like residual contamination by cloud and aerosol, especially when the number of observations to constrain the BRDF model is reduced (e.g. less than 5). The negative impact on the quality of the k_1 and k_2 BRDF coefficients may affect the quality of FAPAR product, causing noisy profiles on a short time scale.

6 References

Bateson, C. A., Asner, G. P., Wessman, C. A. (2000). Endmember bundles: a new approach to incorporating endmember variability into spectral mixture analysis. IEEE Transactions on Geoscience and Remote Sensing, 38, 1083–1094.

Bishop, C.M. (1995), Neural Networks for Pattern Recognition, Oxford:Oxford University Press.

Bosdogianni, P., M. Petrou, and J.Kittler. (1996) Robust mixed pixel classification in remote sensing. In VIII ISPRS-Congress, Vienna, Austria.

Camacho, F., F. Baret, M. Weiss, R. Fernandes, B. Berthelot, J. Sánchez, C. Latorre, J. García-Haro, R. Duca (2013). Validación de algoritmos para la obtención de variables biofísicas con datos Sentinel2 en la ESA: proyecto VALSE-2, XV Congreso de la Asociación Española de Teledetección (AET), Madrid 22-24 de Octubre 2013.

Chen, J. M., C. H. Menges, S. G. Leblanc, (2005), Global mapping of foliage clumping index using multi-angular satellite data, Remote Sensing of Environment, 97: 447 – 457.

Dickinson R.E., 1983: Land surface processes and climate – Surface albedos and energy balance, Adv. Geophys., 25, 305-353.

Diner, D. J., Braswell, B. H., Davies, R., Gobron, N., Hu, J., Jin, Y. (2005). The value of multiangle measurements for retrieving structurally and radiatively consistent properties of clouds, aerosols, and surfaces. Remote Sensing of Environment, 97: 495−518.

Ferranti, L. e P. Viterbo, (2006), The European Summer of 2003: Sensitivity of Soil Water Initial Conditions. J. Climate, 19: 3659-3680.

García-Haro, F.J., Gilabert, M.A., Meliá, J., (1996). Linear spectral mixture modelling to estimate amount of vegetation from optical spectral data. International Journal of Remote Sensing, 17: 3373-3400.

García-Haro, F.J., F. Camacho-de Coca, J. Meliá (2004). Global mapping of vegetation parameters from SEVIRI/MSG data. Remote Sensing for Agriculture, Ecosystem and Hydrology, vol 5233, pp 30-41. Editorial: (SPIE: Bellingham, WA) edited by M. Owe, G. d'Urso, J. Moreno and A.Calera, ISBN 0-8194-5115-0, (Bellingham, WA).

García-Haro, F.J, S. Sommer, T. Kemper (2005a), Variable multiple endmember spectral mixture analysis (VMESMA), International Journal of Remote Sensing, 26:2135-2162.

García-Haro, F.J., F. Camacho-de Coca, J. Meliá, B. Martínez, Operational derivation of vegetation products in the framework of the LSA SAF project, (2005b), in Proceedings of 2005 EUMETSAT Meteorological Satellite Conference. Dubrovnik (Croatia). 19-23 September, (Eumetsat Publ.: Darmstad), ISBN 92-9110-073-0, ISSN 1011-3932, pp 247-254

García-Haro, F. J., Camacho-de Coca, F. and Meliá, J. (2006), Algorithm development and current status of the SEVIRI/MSG LAI and FVC products, Proceedings of the RAQRS'II 2nd International Symposium on Recent Advances in Remote Sensing, 25-29 September 2006, (Publ. Univ. Valencia: Valencia), Ed. J. Sobrino, ISBN: 84-3706554-X, 978-84-370-633-5, pp: 758-763.

García-Haro, F.J., Camacho, F., Martínez, B., Campos-Taberner, M., Grau, G., Sánchez, S., Sánchez, J., Moreno, A., Gilabert, M.A. (2016). The LSA SAF vegetation products, DUE GlobTemperature User Consultation Meeting, 7-8 June 2016, Lisbon (Portugal).

Geiger, B., D. Carrer, L. Franchisteguy, J.L. Roujean, C. Meurey (2008), Land Surface Albedo Derived on a Daily Basis From Meteosat Second Generation Observations, IEEE Transactions on Geoscience and Remote Sensing, 46: 3841-3854.

Hu, J. Y. Su, B. Tan, D. Huang, W. Yang, M. Schull, M.A. Bull, J. V. Martonchik, D. J. Diner, Y. Knyazikhin, R. B. Myneni, (2007). Analysis of the MISR LAI/FPAR product for spatial and temporal coverage, accuracy and consistency, Remote Sensing of Environment 107: 334–347

Huete, A.R. (1988). A Soil Adjusted Vegetation Index (SAVI). Remote Sens Env. 25:295-309.

Knyazikhin, Y., Marshak, A. (2000). Mathematical aspects of BRDF modeling: Adjoint problem and Green's function. Remote Sensing Reviews, 18, 263−280.

Malingreau, J. P., A. S. Belward. (1992). Scale considerations in vegetation monitoring using AVHRR data. International Journal of Remote Sensing. 13:2289-2307.

Mitchell, K., et al., 2004: The multi-institution North American Land Data Assimilation System NLDAS: Utilizing multiple GCIP products and partners in a continental distributed hydrological modeling system, J. Geophys. Res., 109, doi:10.1029/2003JD003823.

National Research Council. 2004. Climate Data Records from Environmental Satellites: Interim Report. Washington, DC: The National Academies Press. https://doi.org/10.17226/10944.

Nilson, T., (1971). A theoretical analysis of the frequency of gaps in plant stands, Agriculture and Meteorology, 8, 25-38.

Roberts, D. A., Gardner, M., & Church, R. (1998). Mapping chaparral in the Santa Monica mountains using multiple endmember spectral mixture models. Remote Sens. Environ., 65, 267–279.

Ross, J.K. (1981),The radiation regime and architecture of plants stands, Norwell, MA: Dr. W. Junk, 391 pp.

Roujean J.-L., M. Leroy and P.-Y. Deschamps, (1992), A bidirectional reflectance model of the Earth's surface for the correction of remote sensing data, J. Geophys. Res., 97(D18), 20455-20468.

Roujean, J.-L. and F.-M. Bréon, (1995). Estimating PAR absorbed by vegetation from Bidirectional Reflectance Measurements. Remote Sensing of Environment, 51: 375-384.

Roujean, J. L., Tanré, D., Bréon, F-M. and Deuzé, J-L. (1997). Retrieval of land surface parameters from airborne POLDER bi-directional reflectance distribution function during HAPEX-Sahel. Journal of Geophysical Research 102(D10), 11 201-11 218.

Roujean, J.L. and R. Lacaze, (2002). Global mapping of vegetation parameters from POLDER multiangular measurements for studies of surface-atmosphere interactions: A pragmatic method and its validation. J. Geophysical Res., 107D, 10129-10145.

Schmetz, J., Pili, P., Tjemkes, S., Just, D., Kerkmann, J., Rota, S., Ratier, A., 2002. An introduction to Meteosat Second Generation (MSG). Bull. Am. Meteorol. Soc. 83, 977–992.

Sellers, P. J., Y. Mintz, Y. C. Sud, and A. Dalcher, 1997: BOREAS in 1997: Experiment overview, scientific results, and future directions. J. Geophys. Res., 102, 28 731–28 769.

Smith N. J., Chen J. M., Black T. A, 1993. Effects on clumping on estimates of stand leaf area index using LI-COR LAI-2000. Can J. For. Res. 23:1940–1943.

Song, C., 2005, Spectral mixture analysis for subpixel vegetation fractions in the urban environment: How to incorporate endmember variability?, Remote Sens. Environ. 95: 248–263.

Verger, A., Camacho-de Coca, F., García-Haro, J., Meliá, J. (2007). Direct validation of FVC, LAI and FAPAR VEGETATION/SPOT derived products using LSA SAF methodology. In Proceedings of IEEE International Geoscience and Remote Sensing symposium, 23-27 July 2007, Barcelona (Spain).

Verger, A., F. Camacho, F. J. García-Haro, J. Meliá (2009a). Prototyping of Land-SAF leaf area index algorithm with VEGETATION and MODIS data over Europe. Remote Sensing of Environment, 113: 2285–2297.

Verger, A., Martínez, B., Camacho-de Coca, F., García-Haro, F. J. (2009b), Accuracy assessment of fraction of vegetation cover and leaf area index estimates from pragmatic methods in a cropland area. International Journal of Remote Sensing. 30:2685–2704.

Verhoef, W., (1984). Light scattering by leaf layers with application to canopy reflectance modeling: the SAIL model. Remote Sens. Environ., 16, 125-141.

Wang, Y., Buermann,W., Stenberg, P., Voipio, P., Smolander, H., Häme, T., et al. (2003). A new parameterization of canopy spectral response to incident solar radiation: Case study with hyperspectral data from pine dominant forest. Remote Sensing of Environment, 85, 304−315.

Weiss, M., F. Baret, R. Myneni, A. Pragnère, and Y. Knyazikhin. (2000). Investigation of a model inversion technique for the estimation of crop characteristics from spectral and directional reflectance data. Agronomie 20:3-22.

Wu. H and Zhao-Liang L, (2009), Scale Issues in Remote Sensing: A Review on Analysis, Processing and Modeling, Sensors; 9(3): 1768–1793.

Appendix A. Developers

The development and implementation have been carried out under the responsibility of the Universitat de València.

Authors: F. Javier García-Haro and Fernando Camacho

Appendix B. Glossary

AL:	Land Surface Albedo Product
ASCAT:	Advanced Scatterometer
AVHRR:	Advanced Very High Resolution Radiometer
BA:	Burnt Area
BHRPAR	Bi-Hemispherical Reflectance integrated over the Photosynthetically Active spectral Region
BRDF:	Bi-directional Reflectance Distribution Function
CDOP:	Continuous Development and Operations Phase
CDR:	Climate Data Record
CWC:	Canopy Water Content
DRR:	Dataset Readiness Review
DSLF:	Down-welling Long-wave Fluxes
DSSF:	Down-welling Short-wave Fluxes
DVI:	Difference Vegetation Index
ECMWF:	European Centre for Medium-Range Weather Forecast
E-M:	Expectation-Maximization
EM:	Land Surface Emissivity
EPS:	EUMETSAT Polar System
ET:	Evapotranspiration
ET0:	Reference Evapotranspiration
EUMETSAT:	European Meteorological Satellite Organisation
FAPAR:	Fraction of Absorbed Photosynthetically Active Radiation
FCI:	Flexible Combined Imager
FD&M:	Fire Detection and Monitoring
FIPAR:	Fraction of solar radiation intercepted by the vegetation
FRE:	Fire Radiative Energy and Emissions
FRM:	Fire Risk Map
FVC:	Fractional Vegetation Cover
GLC:	Global Land Cover
GPP:	Gross Primary Production
HDF:	Hierarchical Data Format
IPMA:	Instituto Português do Mar e da Atmosfera
LAI:	Leaf Area Index
LE&H:	Surface Energy Fluxes: Latent and Sensible
LIFD:	Leaf inclination distribution
LSA:	Land Surface Analysis
LST:	Land Surface Temperature

MERIS:	MEdium Resolution Image Spectrometer Instrument
METEOSAT:	Geostationary Meteorological Satellite
METOP:	Meteorological Operational polar satellites of EUMETSAT
MF:	Météo-France
MIR:	Middle-InfraRed
MISR:	Multi-Angle Imaging Spectra-Radiometer
MODIS:	Moderate-Resolution Imaging Spectro-Radiometer
MSG:	Meteosat Second Generation
MTFAPAR-R :	Meteosat Ten-day FAPAR Reprocessed
MTFVC-R:	Meteosat Ten-day FVC Reprocessed
MTG:	Meteosat Third Generation
MTLAI-R:	Meteosat Ten-day LAI Reprocessed
NAfr:	North Africa
NCSA:	National Center for Supercomputing Applications
NDVI:	Normalized Difference Vegetation Index
NIR:	Near-InfraRed
NWP:	Numerical Weather Prediction
ORR:	Operational Readiness Review
PAR:	Photosynthetically Active Radiation
PCR:	Product Consolidation Review
PDUs:	Product Distribution Units
POLDER:	POLarization and Directionality of Earth Reflectance
QC:	Quality Control
RDVI:	Renormalized Difference Vegetation Index
SAF:	Satellite Application Facility
SAfr:	South Africa
SAIL:	Scattering by Arbitrary Inclined Leaves
SAme:	South America
SEVIRI:	Spinning Enhanced Visible and Infrared Imager
SMA:	Spectral Mixture Analysis
SPOT:	Système Probatoire d'Observation de la Terre
TOC:	Top of Canopy
URD:	User Requirements Document
VEGA:	Vegetation Parameters
VIS:	Visible
WMO	World Meteorological Organization
3MI	Multi-viewing Multi-channel Multi-polarization Imager

Appendix C. HDF5-Attributes

The set of general attributes to be part of all LSA SAF files and their possible values are described in the Table 11.

Table 11. General HDF5 attributes of the files for the SEVIRI VEGA products.

Attribute	Description	Data Type	Allowed Values

Attribute	Description	Data Type	Allowed Values
SAF	SAF package	String	LSA
CENTRE	Institution (generating/disseminating data)	String	IM-PT
ARCHIVE_FACILITY	Centre where the data is archived	String	IM-PT
PRODUCT	Defines the name of the product	String	FVC,LAI,FAPAR
PARENT_PRODUCT_NAME	Array of up to 4 product names, upon which the product is based	String Array(4)	AL-K012
SPECTRAL_CHANNEL_ID	Channel Identification	Int	768
PRODUCT_ALGORITHM_VERSION	Version of the Algorithm that produce the product	String	X.Y
CLOUD_COVERAGE	Indicator of the cloud coverage in the product	String	NWC-CMA
OVERALL_QUALITY_FLAG	Overall quality flag for the product	String	OK
ASSOCIATED_QUALITY_INFORMATION	Several miscellaneous quality indicator for the product	String	-
REGION_NAME	Processed Region Name	String	One of: Euro, NAfr, SAfr, SAme, MSG-Disk
COMPRESSION	Compression Flag	Int	0 (Uncompressed)
FIELD_TYPE	Data filed type	String	Product
FORECAST_STEP	Forecast Step in Hours	Integer	0
NC	Maximum number of columns for the variables to read/write	Int	Depend on region name
NL	Maximum number of lines for the variables to read/write	Int	Depend on region name
NB_PARAMETERS	Number of variables to read/write	Int	3
NOMINAL PRODUCT_TIME	Nominal Time of the Product	String	YYMMDDhhmmss
SATELLITE	Satellite Identification	String	MSG1, MSG2, MSG3,…
INSTRUMENT_ID	Instrument which acquired the product or data used by the product	String	SEVI
INSTRUMENT_MODE	Scanning mode of the instrument at the time of the acquisition	String	STATIC_VIEW
IMAGE_ACQUISITION_TIME	Image Acquisition Time (SEVIRI 1.5 Images)	String	YYMMDDhhmmss
ORBIT_TYPE	Coverage of the product (only for EPS)	String	GEO
PROJECTION_NAME	Projection name and sub-satellite point	String	Geos<sub_lon> (as from SEVIRI 1.5 Images)
NOMINAL_LONG	Satellite Nominal Longitude	Real	As from SEVIRI 1.5 Images
NOMINAL_LAT	Satellite Nominal Latitude	Real	As from SEVIRI 1.5 Images

Attribute	Description	Data Type	Allowed Values
CFAC	Column Scaling Factor (SEVIRI 1.5 Images)	Int	As from SEVIRI 1.5 Images
LFAC	Line Scaling Factor (SEVIRI 1.5 Images)	Int	As from SEVIRI 1.5 Images
COFF	Column Offset (SEVIRI 1.5 Images)	Int	As from SEVIRI 1.5 Images
LOFF	Line Offset (SEVIRI 1.5 Images)	Int	As from SEVIRI 1.5 Images
START_ORBIT_NUMBER	First of two orbit numbers in the EPS product, valid at the starting of the sensing, i.e, at the beginning of a dump	Int	0
END_ORBIT_NUMBER	Final of the orbit numbers in the EPS product, valid at the ascending node crossing, i.e. towards the end of a dump	Int	0
SUB_SATELLITE_POINT_START_LAT	Latitude of sub-satellite at start of acquisition	Real	0.0
SUB_SATELLITE_POINT_START_LON	Longitude of sub-satellite at start of acquisition	Real	0.0
SUB_SATELLITE_POINT_END_LAT	Latitude of sub-satellite at end of acquisition	Real	0.0
SUB_SATELLITE_POINT_END_LON	Longitude of sub-satellite at end of acquisition	Real	0.0
SENSING_START_TIME	UTC date & time at acquisitions start of the product	String	YYMMDDhhmmss
SENSING_END_TIME	UTC date & time at acquisition end of the product	String	YYMMDDhhmmss
PIXEL_SIZE	For image products, size of pixel at nadir. For meteorological products resolution/accuracy	String	3.1Km
GRANULE_TYPE	Type description of the item	String	DP
PROCESSING_LEVEL	Processing Level Applied for generation of the product	String	0.2
PRODUCT_TYPE	Abbreviation name for the product type rather product category	String	LSAFVC,LSALAI,LSAFAPAR
PRODUCT_ACTUAL_SIZE	Actual size of the product	String	Depends on the region
PROCESSING_MODE	Processing mode for generation of the product	String	N
DISPOSITION_FLAG	Disposition status indicator of the product, as set by the UMARF operator	String	O
TIME_RANGE	Temporal Resolution	String	Daily , 10-day
STATISTIC_TYPE	Statistic Type	String	-
MEAN_SSLAT		Real	Depend on REGION_NAME
MEAN_SSLON		Real	Depend on REGION_NAME
PLANNED_CHAN_PROCESSING		Integer	0

Attribute	Description	Data Type	Allowed Values
FIRST_LAT		Real	0
FIRST_LON		Real	0

LSB – Lower Significant Bit
MSB – Most Significant Bit
YY - Year; MM-Month; DD – Day; hh – Hour; mm – Minute; ss – Second
String => Character (len=80)
Int => Integer (kind=4)
Real => Real (kind=8)

The attributes for each dataset of the HDF5-files are described in table 12.

Table 12. Dataset atributes.

Attribute	Description	Data Type	Value for VEGA datasets	Value for VEGA Error datasets	Value for Q-Flag datasets
CLASS	Dataset type	String	Data	Data	Data
PRODUCT	Defines the name of the product	String	FVC LAI FAPAR	FVC err LAI err FAPAR err	FVC QF LAI QF FAPAR QF
PRODUCT_ID	Product identification accordingly with WMO tables	Integer			
N_ COLS	Number of columns	Integer	Depend on REGION_NAME (Table 4)	Depend on REGION_NAME (Table 4)	Depend on REGION_NAME (Table 4)
N_ LINES	Number of lines	Integer	Depend on REGION_NAME (Table 4)	Depend on REGION_NAME (Table 4)	Depend on REGION_NAME (Table 4)
NB_BYTES	Number of bytes per pixel	Integer	2	2	1
SCALING_FACTOR	Scaling factor for the parameter	Real	10000 for FVC 10000 for FAPAR 1000 for LAI	10000 for FVC 10000 for FAPAR 1000 for LAI	1.0
OFFSET	Offset of the scaling factor	Real	0.0	0.0	0.0
MISS_VALUE	Missing value	Integer	-10	-10, -15, -20, -30, -31, -40, -50 or -60	N/A
UNITS	Parameter Unities	Integer	1	1	N/A
CAL_SLOPE	Calibration Constant	Real	1.0	1.0	1.0
CAL_OFFSET	Calibration Constant	Real	0.0	0.0	0.0